The Polarizing Sagnac Interferometer: a tool for light orbital angular momentum sorting and spin-orbit photon processing

S. Slussarenko,[1] V. D'Ambrosio,[1] B. Piccirillo,[1,2] L. Marrucci,[1,3] and E. Santamato[1,2,*]

[1]*Dipartimento di Scienze Fisiche, Università di Napoli "Federico II", Complesso Universitario di Monte S. Angelo, 80126 Napoli, Italy*

[2]*CNISM-Consorzio Nazionale Interuniversitario per le Scienze Fisiche della Materia, Napoli, Italy*

[3]*CNR-SPIN, Complesso Universitario di Monte S. Angelo, 80126 Napoli, Italy*

**enrico.santamato@na.infn.it*

Abstract: In this paper we show that an optical setup based on a polarizing Sagnac interferometer combined with a Dove prism can be used as a convenient general-purpose tool for the generation, detection and sorting of spin-orbit states of light. This device can work both in the classical and in the quantum single-photon regime, provides higher sorting efficiency and extinction ratio than usual hologram-fiber combinations, and shows much higher stability and ease of alignment than Mach-Zehnder interferometer setups. To demonstrate the full potential of this setup, we also report some demonstrative experiments of several possible applications of this setup.

OCIS codes: (050.4865) Optical vortices;(270.5585) Quantum information and processing; (120.3180) Interferometry.

References and links

1. M. J. Padgett and J. P. Lesso, "Dove prisms and polarized light," J. Mod. Opt. **46**, 175–179 (1999).
2. G. P. I. Moreno and M. Strojnik, "Polarization transforming properties of dove prisms," Opt. Commun. **220**, 257-268 (2003).
3. I. Moreno, "Jones matrix for image-rotation prisms," Appl. Opt. **43**, 3373-3381 (2004).
4. L. Allen, M. W. Beijersbergen, R. J. C. Spreeuw, and J. P. Woerdman, "Orbital angular momentum of light and the transformation of Laguerre-Gaussian laser modes," Phys. Rev. A **45**, 8185–8189 (1992).
5. L. Allen, S. M. Barnett, and M. J. Padgett, eds., *Optical angular momentum* (Institute of Physics Publishing, Bristol, 2003).
6. G. Molina-Terriza, J. P. Torres, and L. Torner, "Twisted photons," Nat. Phys. **3**, 305–310 (2007).
7. S. Franke-Arnold, L. Allen, and M. Padgett, "Advances in optical angular momentum," Laser Photon. Rev. **2**, 299–313 (2008).
8. A. V. Sergienko, *Quantum Communications and Cryptography* (Taylor & Francis Group, 2006).
9. G. Molina-Terriza, J. P. Torres, and L. Torner, "Management of the angular momentum of light: Preparation of photons in multidimensional vector states of angular momentum," Phys. Rev. Lett. **88**, 013601 (2002).
10. G. Molina-Terriza, A. Vaziri, J. Rehacek, Z. Hradil, and A. Zeilinger, "Triggered qutrits for quantum communication protocols," Phys. Rev. Lett. **92**, 167903 (2004).
11. G. Gibson, J. Courtial, M. J. Padgett, M. Vasnetsov, V. Pasko, S. M. Barnett, and S. Franke-Arnold, "Free-space information transfer using light beams carrying orbital angular momentum," Opt. Express **12**, 5448–5456 (2004).
12. D. Kaszlikowski, P. Gnacinski, M. Zukowski, W. Miklaszewski, and A. Zeilinger, "Violations of local realism by two entangled n-dimensional systems are stronger than for two qubits," Phys. Rev. Lett. **85**, 4418–4421 (2000).
13. V. Karimipour, A. Bahraminasab, and S. Bagherinezhad, "Quantum key distribution for *d*-level systems with generalized bell states," Phys. Rev. A **65**, 042320 (2002).

#132709 - $15.00 USD Received 2 Aug 2010; revised 9 Sep 2010; accepted 7 Oct 2010; published 10 Dec 2010

14. N. J. Cerf, M. Bourennane, A. Karlsson, and N. Gisin, "Security of quantum key distribution using d-level systems," Phys. Rev. Lett. **88**, 127902 (2002).
15. B. P. Lanyon, M. Barbieri, M. P. Almeida, T. Jennewein, T. C. Ralph, K. J. Resch, G. J. Pryde, J. L. O'Brien, A. Gilchrist, and A. G. White, "Simplifying quantum logic using higher-dimensional hilbert spaces," Nat. Phys. **5**, 134–140 (2009).
16. T. Vértesi, S. Pironio, and N. Brunner, "Closing the detection loophole in bell experiments using qudits," Phys. Rev. Lett. **104**, 060401 (2010).
17. This is strictly true for paraxial beams only.
18. E. Nagali, L. Sansoni, F. Sciarrino, F. D. Martini, L. Marrucci, B. Piccirillo, E. Karimi, and E. Santamato, "Optimal quantum cloning of orbital angular momentum photon qubits through hong-ou-mandel coalescence," Nat. Photon. **3**, 720–723 (2009).
19. E. Nagali, F. Sciarrino, F. D. Martini, L. Marrucci, B. Piccirillo, E. Karimi, and E. Santamato, "Quantum information transfer from spin to orbital angular momentum of photons," Phys. Rev. Lett. **103**, 013601 (2009).
20. E. Nagali, F. Sciarrino, F. D. Martini, B. Piccirillo, E. Karimi, L. Marrucci, and E. Santamato, "Polarization control of single photon quantum orbital angular momentum states," Opt. Express **17**, 18745–18759 (2009).
21. E. Nagali, L. Sansoni, L. Marrucci, E. Santamato, and F. Sciarrino, "Experimental generation and characterization of single-photon hybrid ququarts based on polarization and orbital angular momentum encoding," Phys. Rev. A **81**, 052317 (2010).
22. E. Nagali, D. Giovannini, L. Marrucci, S. Slussarenko, E. Santamato, and F. Sciarrino, "Experimental optimal cloning of four-dimensional quantum states of photons," Phys. Rev. Lett. **105**, 073602 (2010).
23. V. Y. Bazhenov, M. V. Vasnetsov, and M. S. Soskin, "Laser beams with screw dislocations in their wavefronts," Sov. Phys.–JETP Lett. **52**, 429–431 (1990).
24. J. Leach, M. J. Padgett, S. M. Barnett, S. Franke-Arnold, and J. Courtial, "Measuring the orbital angular momentum of a single photon," Phys. Rev. Lett. **88**, 257901 (2002).
25. J. Leach, J. Courtial, K. Skeldon, S. M. Barnett, S. Franke-Arnold, and M. J. Padgett, "Interferometric methods to measure orbital and spin, or the total angular momentum of a single photon," Phys. Rev. Lett. **92**, 013601 (2004).
26. M. J. Padgett and L. Allen, "Orbital angular momentum exchange in cylindrical-lens mode converters," J. Opt. B: Quantum Semiclassical Opt. **4**, S17–S19 (2002).
27. L. Marrucci, C. Manzo, and D. Paparo, "Optical spin-to-orbital angular momentum conversion in inhomogeneous anisotropic media," Phys. Rev. Lett. **96**, 163905 (2006).
28. L. Marrucci, C. Manzo, and D. Paparo, "Pancharatnam-Berry phase optical elements for wavefront shaping in the visible domain: switchable helical modes generation," Appl. Phys. Lett. **88**, 221102 (2006).
29. Suitable waveplates can be introduced to compensate the polarization change introduced by real Dove prism, but this is often unnecessary because the polarization change is very small [1–3].
30. E. Karimi, S. Slussarenko, B. Piccirillo, L. Marrucci, and E. Santamato, "Polarization-controlled evolution of light transverse modes and associated pancharatnam geometric phase in orbital angular momentum," Phys. Rev. A **81**, 053813 (2010).
31. Examples are the diagonal, antidiagonal, left-circular, right-circular polarizations.
32. M. Frede, R. Wilhelm, M. Brendel, C. Fallnich, F. Seifert, B. Willke, and K. Danzmann, "High power fundamental mode nd:yag laser with efficient birefringence compensation," Opt. Express **12**, 3581–3589 (2004).
33. E. A. Khazanov, O. V. Kulagin, S. Yoshida, D. B. Tanner, and D. H. Reitze, "Investigation of self-induced depolarization of laser radiation in terbium gallium garnet," IEEE J. Quantum Electron. **35**, 1116–1122 (1999).
34. N. F. Andreev, O. V. Palashov, A. K. Potemkin, D. H. Reitze, A. M. Sergeev, and E. A. Khazanov, "A 45-db faraday isolator for 100-w average radiation power," Quantum Electron. **30**, 1107–1108 (2000).
35. If the pure OAM eigenstates $|\ell\rangle$ are described by Laguerre-Gaussian modes, then the $|h_\ell\rangle$ and $|v_\ell\rangle$ states correspond to Hermite-Gaussian modes.
36. M. Fiorentino and F. N. Wong, "Deterministic controlled-not gate for single-photon two-qubit quantum logic," Phys. Rev. Lett. **93**, 070502 (2004).
37. L. Hardy, "Non locality for two particles without inequalities for almost all entangled states," Phys. Rev. Lett. **71**, 1665–1668 (1993).
38. E. Karimi, B. Piccirillo, L. Marrucci, and E. Santamato, "Light propagation in a birefringent plate with topological charge," Opt. Lett. **34**, 1225–1227 (2009).
39. N. González, G. Molina-Terriza, and J. P. Torres, "How a dove prism transforms the orbital angular momentum of a light beam," Opt. Express **14**, 9093–9102 (2006).
40. D. F. V. James, P. G. Kwiat, W. J. Munro, and A. G. White, "Measurement of qu-bit," Phys. Rev. A **64**, 052312 (2001).
41. M. J. Padgett and J. Courtial, "Poincaré-sphere equivalent for light beams containing orbital angular momentum," Opt. Lett. **24**, 430–432 (1999).

#132709 - $15.00 USD Received 2 Aug 2010; revised 9 Sep 2010; accepted 7 Oct 2010; published 10 Dec 2010

1. Introduction

It is well known that photons can carry two different types of angular momenta: the spin angular momentum (SAM), associated with the light polarization, and the orbital angular momentum (OAM), associated with the azimuthal distribution of the complex electrical field [4–7]. A circularly polarized beam carries $\sigma\hbar$ SAM per photon, where $\sigma = \pm 1$ corresponds to the handedness of polarization. A beam with azimuthal phase dependence of $\exp(i\ell\phi)$ (where ϕ is transverse azimuthal angular coordinate and ℓ is an integer) carries a definite OAM $\ell\hbar$ per photon [4]. SAM forms a two-dimensional Hilbert space and is one of the most used physical realizations of a qubit – fundamental unit in quantum information and cryptography [8]. The OAM space, instead, is inherently multidimensional and thus can be used for realization of qudits, i.e. multilevel (more than two) quantum states [9, 10]. Qudits are useful for increasing of the total amount of information carried by single photon [10, 11], or to implement more complex quantum computation algorithms and protocols not applicable in the binary polarization space (see, e.g., Refs. [12–16]). The SAM and OAM spaces of the same photon, being independent from each other [17], can be used together for creating single-photon entangled (or non-separable) quantum states, including qudits [18–22]. Sorting photons according to their different polarization states is very easily accomplished by polarizing beamsplitters and birefringent waveplates. Sorting photons according to their different OAM modes is a more complex problem, although a number of techniques have been conceived to this purpose [23–26]. A very common technique to detect single photon OAM is based on "fork-like" computer-generated holograms used in combination with suitable pinhole or single-mode optical-fiber mode filtering [23]. However, this technique is affected by the low overall transmission efficiencies of the hologram and of the optical fiber (or pinhole) filtering system. Rarely the overall efficiency of such systems can exceed 40%. Alternative setups involve a Mach-Zehnder interferometer with two Dove prisms [24, 25] or two confocal cylindrical lenses acting as OAM mode converters [26]. These techniques have a theoretical efficiency of 100% and may be used in the single photon regime, but require high mechanical stability, careful path matching of the arms of the interferometer and careful positioning and alignment of the cylindrical lenses, which makes them not very practical.

In this paper, we propose a novel OAM sorting interferometric setup based on a polarizing Sagnac interferometer (PSI) and a single Dove prism (DP). This setup, labeled PSI-DP in the following, ideally has a 100% efficiency, works with single photons, and has a good stability because of the self-compensation of the optical paths inside the interferometer. Moreover, the use of a single Dove prism further simplifies the setup. In the following, we will discuss and demonstrate experimentally the ability of the PSI-DP to sort photons carrying different OAM values, and will present some additional demonstrative applications of the PSI-DP in spin-orbit processing, such as the realization of a C-NOT gate, efficient photon spin-orbit Bell's states measurement and entanglement control of the spin-orbit Schmidt's state – a two-component non-maximally entangled state in the spin-orbit Hilbert space. These experiments required photons in definite OAM eigenstates that were generated and analyzed by means of auxiliary setups based on the q-plate (QP), a newly introduced device able to convert the photon spin into OAM by the spin-to-orbital conversion (STOC) process [27, 28]. A brief overview of the QP and its action on the photon OAM is given in the experimental section below.

2. The Polarizing Sagnac Interferometer

Interferometer-based OAM sorting methods usually exploit the $\exp(i\ell\phi)$ spiraling phase form of the light beams carrying a definite value of OAM. When such beams are rotated around their axis through an angle α, the wavefront phase dependence changes into $\exp(i\ell(\phi+\alpha))$, so that a phase shift $\Delta\psi = \ell\alpha$ appears in the rotated beam. A device, that may be used to in-

#132709 - $15.00 USD Received 2 Aug 2010; revised 9 Sep 2010; accepted 7 Oct 2010; published 10 Dec 2010

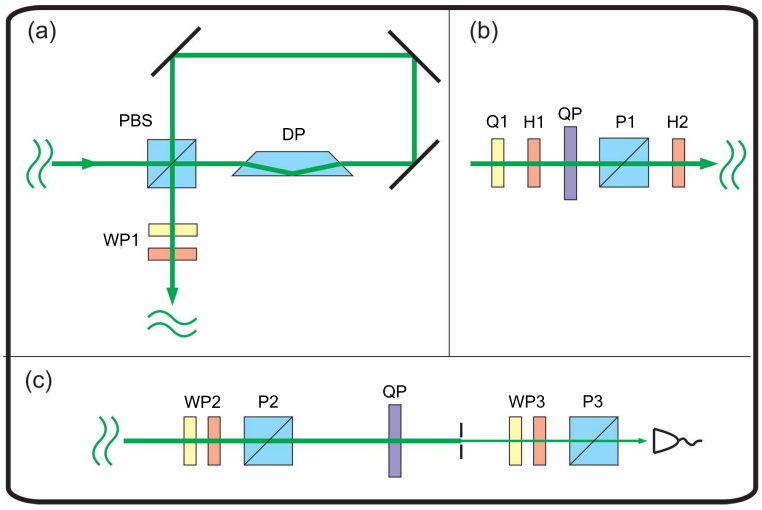

Fig. 1. (a) the polarizing Sagnac interferometer (PSI) with Dove prism (DP), or PSI-DP. (b) The auxiliary setup used to generate photons with OAM $\ell = \pm 2$. Some of the optical components were eventually placed or removed to create the input states for each experimental demonstration. (c) The auxiliary setup used to analyze photons with OAM $\ell = \pm 2$. The auxiliary setups in (b) and (c) use a q-plate (QP) to convert the photon spin into OAM and viceversa. Legenda of other symbols: PBS - polarizing beam-splitter; WP - generic waveplate; Q - quarter-wave plate; H - half-wave plate; P - polarizer.

duce such beam rotation is the DP. The DP flips the transverse cross section of the transmitted beam, so that two DPs, rotated at angle α with respect to each other induce an overall rotation of the transverse optical field of an angle 2α along the beam axis. DPs are commonly used in periscopes to maintain the image right when the periscope is rotated. As suggested by Leach [24] two DPs inserted in the arms of a Mach-Zehnder interferometer can be used to sort the incident photons according to their OAM. Here we used a single DP, instead, inserted in a PSI as shown in Fig. 1(a).

A single polarizing beam splitter (PBS) is used as entry and exit gate of the device. The PBS splits the incident beam into its horizontal ($|H\rangle$) and vertical ($|V\rangle$) components which circulate inside the interferometer along the same path, but in the opposite directions. After being reflected by the mirrors they recombine again and exit the interferometer from the other side of the PBS. Inserting in the PSI a single DP rotated through an angle α with respect to the interferometer plane is equivalent to inserting two DPs in the two arms of the Leach interferometer, rotated with respect of each other through an angle 2α. After passing through the interferometer, the two counter-propagating orthogonal polarizations $|H\rangle$ and $|V\rangle$ will gain a relative phase of $4\ell\alpha$. In this way, our setup is able to induce an ℓ-dependent change of the polarization state of the incident beam. The OAM sign remains unchanged, however, because the total number of reflections from mirrors, PBS, and DP is even for both polarizations. Neglecting scattering and absorption losses and assuming an ideal polarization preserving Dove prism [29], the theoretical transparency of the PSI-DP device is 100%. As shown in the next section, the PSI-DP can simulate the Leach interferometer for OAM photon sorting. But it should be noticed that the PSI-DP handles polarization too, so it can perform a wider set of operations in the OAM and also in the full photon spin-orbit space. For example, when qubits formed by opposite OAM eigenstates $|\pm\ell\rangle$ are considered, the PSI-DP may simulate a $\pi/2$ cylindrical lens converter, changing LG_ℓ modes into HG_ℓ modes [30]. The capability of doing complex operations in the

#132709 - $15.00 USD Received 2 Aug 2010; revised 9 Sep 2010; accepted 7 Oct 2010; published 10 Dec 2010

photon spin-orbit space, the need of a single Dove prism, and the robustness with respect mechanical solicitations due to the optical path self-compensation render the PSI-DP much more attractive than conventional Mach Zehnder- based interferometers in all applications were the photon OAM plays an important role. In the remaining part of this work, we will discuss some possible practical applications of the PSI-DP device, in order to demonstrate its potential.

2.1. The OAM sorter

The ℓ-dependent relative phase shift induced by the PSI-DP can be exploited for sorting input photons sharing the same polarization state according to their different OAM values into orthogonal polarization states of the exit beam. The further separation over different paths is then easily and efficiently accomplished by suitable waveplates and PBS. Let us assume the impinging photon having a definite value ℓ of OAM and definite polarization state $|\psi\rangle = a|H\rangle + b|V\rangle$. The input photon state is denoted by $|\psi,\ell\rangle$, where the first slot in the ket denotes the polarization state and the second slot the OAM state. The action of the PSI-DP with DP at angle α on such a photon state is given by

$$|\psi,\ell\rangle \xrightarrow{\widehat{PSI_\alpha}} ae^{2i\ell\alpha}|H,\ell\rangle + be^{-2i\ell\alpha}|V,\ell\rangle = -i\cos 2\ell\alpha|\psi,\ell\rangle + \sin 2\ell\alpha|\psi',\ell\rangle) \tag{1}$$

where $|\psi'\rangle = a|H\rangle - b|V\rangle$. We see that for input states with equally weighted H and V polarizations (i.e. states with $|a|^2 = |b|^2 = 1/2$), the states $|\psi'\rangle$ and $|\psi\rangle$ are orthogonal, so that they can be easily separated. In this work we assume always equally weighted input polarization states [31]. Then, from Eq. (1) we see that if $2\ell\alpha = k\pi$ (integer k) the polarization state remains unchanged (up to a global phase factor), while if $2\ell\alpha = \pi/2 + k\pi$ the polarization state becomes orthogonal to the incident one. Setting, for example, the angle of the DP to $\alpha = \pi/4$ the PSI-DP changes the polarization of the photons that carry odd values of OAM to the orthogonal state $|\psi'\rangle$, while the photons that carry even values of OAM remain in their $|\psi\rangle$ polarization state. Using a half-wave plate (HWP), with optical axis rotated through an angle of $\pi/8$, and a PBS placed after the PSI-DP, the even and odd values of OAM are spatially separated for detection purposes. One or more cascaded PSI-DPs may work as an OAM eigenstates sorter in the same way as the Leach interferometer [24, 25]. As the Leach interferometer, the PSI-DP works in the single-photon regime and has nominal 100% transmission efficiency. The main advantages of the PSI-DP are the use of a single DP and the self-compensation of the optical paths so that no adjustments are required to obtain destructive interference. Unlike the Leach interferometer, however, the PSI-DP handles the OAM content of the two orthogonal polarizations in a different way. This peculiar feature can be exploited for applications different from the OAM photon sorting. A few examples are outlined below.

2.1.1. OAM qubit measurement

In many quantum optics experiments dealing with photon SAM and OAM, the OAM space is restricted to only two OAM eigenstates given in advance. This is due to the fact that two given eigenstates of a quantum system provide a qubit – the minimal unit of quantum information. Unlike in the photon spin case, however, where the two states have opposite eigenvalues, in the case of photon OAM we may form qubits with any pair of eigenvalues ℓ_1 and ℓ_2. Qubits must be created and than analyzed and detected. In the detection stage, different qubits must be sorted and sent onto different channels. In the case of the photon SAM this task is accomplished by a PBS. In the case of photon OAM qubits, this task is usually performed by suitable computer generated holograms (see [6, 7] and references therein), whose efficiency rarely exceeds 40%. The OAM photon sorting can be accomplished with greater efficiency by the PSI-DP exploiting the ℓ-dependent relative phase shift to address photons with any prescribed pair of OAM values

#132709 - $15.00 USD Received 2 Aug 2010; revised 9 Sep 2010; accepted 7 Oct 2010; published 10 Dec 2010

ℓ_1 and ℓ_2 into orthogonal polarization states of the exit beam. In fact, evaluating Eq. (1) for $\ell = \ell_1$ and $\ell = \ell_2$ and imposing that the output polarization states are orthogonal, we find the condition

$$\cos 2(\ell_2 - \ell_1)\alpha = 0 \;\; \Rightarrow \;\; \alpha = \frac{(2k+1)\pi}{4(\ell_2 - \ell_1)} \tag{2}$$

with integer *k*. In most quantum optics experiments, OAM states with opposite values of ℓ are prescribed. To discriminate the states $|+\ell\rangle$ and $|-\ell\rangle$, the DP must be set at $\alpha = \pi/8\ell$. The two orthogonal polarizations at the PSI-DP output are then sent into different paths by conventional PBS. When configured in this way, the PSI-DP behaves as an OAM beam-splitter. The contrast ratio and overall transmission are limited only by constructive defects, so they may be very large as shown in the experimental section.

2.1.2. OAM subspace purification

As said above, in many quantum applications qubits are formed combining the $|+\ell\rangle$ and $|-\ell\rangle$ OAM eigenstates, as they are not affected by Gouy dephasing effects [19]. In these cases, it may be of some importance to clean up the beam from all other OAM components. Because the OAM eigenstates are usually originated from TEM_{00} laser beams, it is of particular interest to clean up the beam from any residual $\ell = 0$ OAM component. The PSI-DP can be used to this purpose by simply setting the angle of the DP at $\alpha = \pi/(4\ell)$ and polarizing the input photon along the antidiagonal direction. In fact, when Eq. (1) with $\alpha = \pi/(4\ell)$ is applied to the qutrit $|\psi_{in}\rangle = a|A,0\rangle + b|A,-\ell\rangle + c|A,\ell\rangle$ we obtain the output state $|\psi_{out}\rangle$ as

$$|\psi_{out}\rangle = -ia|A,0\rangle + b|D,-\ell\rangle - c|D,\ell\rangle, \tag{3}$$

so that the input $\ell = 0$ component is left in its initial antidiagonal polarization state and the two $\pm\ell$ components are put into the orthogonal diagonal polarization state. The $\ell = 0$ component can be then easily separated from the ℓ and $-\ell$ by a PBS placed at the output port of the device. Such $\ell = 0$ filtering is very useful since most holograms, spiral phase plates, q-plates etc., commonly used to generate OAM eigenvalues from TEM_{00} beam, do not produce OAM eigenstates with 100% purity due to misalignment and inaccuracies of fabrication. It is worth noting that the $\ell = 0$ component of the input beam is not lost, but sent into one output port of the final PBS. We may then use the same device to filter out the nonzero OAM components leaving a very pure output TEM_{00} mode with no losses. This can be useful, for example, to face the serious problem of combining high power ($\simeq$ 100 W or more) with excellent beam quality, as e.g. in lasers systems [32] and Faraday isolators [33, 34] currently developed for gravitational wave detection.

2.2. Spin-orbit quantum computation

Entangled non-separable photon spin-orbit states are at the core of many quantum information applications. Such states do not show the most notable property of entangled photon pairs – non-locality – nevertheless they exhibit paradoxical quantum features related to the quantum contextuality which render these single-photon entangled states very interesting for quantum computation purposes. In fact, operations like universal unitary gates, deterministic complete Bell measurement, etc., which are impossible in the two-photon case, can be realized in the case of single photons with entangled degrees of freedom. Our PSI-DP acts on the photon SAM and OAM simultaneously, so that it can realize some of the most important gates in the photon spin-orbit space, such as the C-NOT gate, the unitary gate for Bell's states measurement or a gate to generate spin-orbit states with controllable entanglement.

#132709 - $15.00 USD Received 2 Aug 2010; revised 9 Sep 2010; accepted 7 Oct 2010; published 10 Dec 2010

2.2.1. C-NOT gate

The controlled-NOT (C-NOT) gate is the key gate for most of the quantum algorithms based on two qubits. In fact, using C-NOT gates and global phase retarders it is possible to realize any unitary gate in the 4D two-qubit Hilbert space. The C-NOT gate flips the state of one of the qubits depending on the state of the other. If the logical basis of the two-qubit state is given by the four kets $|0,0\rangle$, $|0,1\rangle$, $|1,0\rangle$ and $|1,1\rangle$ and the first qubit is the control one, then the C-NOT gate action performs the following logical operation

$$|0,0\rangle \overset{\widehat{CNOT}}{\longrightarrow} |0,0\rangle; \quad |0,1\rangle \overset{\widehat{CNOT}}{\longrightarrow} |0,1\rangle; \quad |1,0\rangle \overset{\widehat{CNOT}}{\longrightarrow} |1,1\rangle; \quad |1,1\rangle \overset{\widehat{CNOT}}{\longrightarrow} |1,0\rangle. \tag{4}$$

If the spin-orbit space logical basis is given by $|R,-\ell\rangle$, $|R,\ell\rangle$, $|L,-\ell\rangle$ and $|L,\ell\rangle$, where L and R denote the left and right circular polarizations, the PSI-DP with the DP angle set to $\pi/8\ell$ performs an OAM C-NOT operation, changing the polarization state of the photons with OAM $+\ell$ into the orthogonal one and leaving the polarization of the photons with $-\ell$ unchanged. The exit polarization is transformed as $|R\rangle \longrightarrow |A\rangle$, $|L\rangle \longrightarrow |D\rangle$ for the negative OAM value and $|R\rangle \longrightarrow |D\rangle$, $|L\rangle \longrightarrow |A\rangle$ for the positive OAM value. To come back into the circular basis an additional quarter-wave plate with its optical axis oriented at 90° is needed beyond the PSI-DP so that the overall operation is given by

$$\begin{aligned} |L,\ell\rangle &\overset{\widehat{CNOT+QWP}}{\longrightarrow} |L,\ell\rangle; \quad |L,-\ell\rangle \overset{\widehat{CNOT+QWP}}{\longrightarrow} |R,-\ell\rangle; \\ |R,\ell\rangle &\overset{\widehat{CNOT+QWP}}{\longrightarrow} |R,\ell\rangle; \quad |R,-\ell\rangle \overset{\widehat{CNOT+QWP}}{\longrightarrow} |L,-\ell\rangle \end{aligned} \tag{5}$$

The PSI-DP behaves as a C-NOT gate with the polarization as control qubit, if we take as logical basis the states $|H,h_\ell\rangle$, $|H,v_\ell\rangle$, $|V,h_\ell\rangle$ and $|V,v_\ell\rangle$, where $|h_\ell\rangle = (|\ell\rangle + |-\ell\rangle)/\sqrt{2}$ and $|v_\ell\rangle = (|\ell\rangle - |-\ell\rangle)/i\sqrt{2}$ are the superpositions of OAM states, equivalent to the horizontal and vertical polarization states [35]. In this case the OAM state of the $|H\rangle$ and $|V\rangle$ component will be rotated through an angle of $\pm\pi/4\ell$ respectively and the state of the outgoing photon is given by

$$\begin{aligned} |V,v_\ell\rangle &\overset{\widehat{CNOT}}{\longrightarrow} |V,d_\ell\rangle \overset{\widehat{DP}}{\longrightarrow} |V,v_\ell\rangle; \quad |V,h_\ell\rangle \overset{\widehat{CNOT}}{\longrightarrow} |V,a_\ell\rangle \overset{\widehat{DP}}{\longrightarrow} |V,h_\ell\rangle \\ |H,v_\ell\rangle &\overset{\widehat{CNOT}}{\longrightarrow} |H,a_\ell\rangle \overset{\widehat{DP}}{\longrightarrow} |H,h_\ell\rangle \quad |H,h_\ell\rangle \overset{\widehat{CNOT}}{\longrightarrow} |H,d_\ell\rangle \overset{\widehat{DP}}{\longrightarrow} |H,v_\ell\rangle, \end{aligned} \tag{6}$$

where $|a_\ell\rangle$ and $|d_\ell\rangle$ are the OAM states equivalent to the antidiagonal and diagonal polarization states. The final transformation $|d_\ell\rangle \rightarrow |v_\ell\rangle$ and $|a_\ell\rangle \rightarrow |h_\ell\rangle$ to return back into the initial basis is done by a second DP rotated at angle $\pi/8\ell$, placed beyond the PSI-DP. The use of the PSI-DP as a polarization C-NOT gate in the photon polarization-path space was already reported [36].

2.2.2. Bell's states measurements

A well known theorem forbids deterministic and 100% efficient detection of all the four Bell's states of a photon pair with a process that involves just linear optics. Up to now, the experimental realization of the Bell's states detection involves additional degrees of freedom, higher order entanglement, or give probabilistic result with non-unit fidelity. The situation is different in the case of single-particle entanglement, where such measurement is possible. The PSI-DP with a DP oriented at angle $\pi/8\ell$ realizes an unitary optical gate which transforms each one of the four Bell states

$$\begin{aligned} |B_1\rangle &= (|H,h_\ell\rangle + |V,v_\ell\rangle)/\sqrt{2}; \qquad |B_2\rangle = (|H,h_\ell\rangle - |V,v_\ell\rangle)/\sqrt{2}; \\ |B_3\rangle &= (|H,v_\ell\rangle + |V,h_\ell\rangle)/\sqrt{2}; \qquad |B_4\rangle = (|H,v_\ell\rangle - |V,h_\ell\rangle)/\sqrt{2} \end{aligned}$$

#132709 - $15.00 USD Received 2 Aug 2010; revised 9 Sep 2010; accepted 7 Oct 2010; published 10 Dec 2010

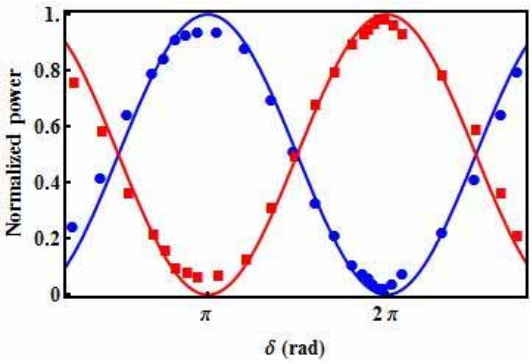

Fig. 2. Filtering the TEM_{00} mode from the OAM carrying beam. Squares ($\ell = 2$) and dots ($\ell = 0$) represent the normalized intensities of the two exits of the final PBS $P2$ in Fig. 1(c), as functions of the QP optical retardation δ. The solid curves are best fits with $\sin^2 \delta/2$ and $\cos^2 \delta/2$ behavior expected from Eq. (8). The experiment was repeated for $\ell = -2$ with similar results.

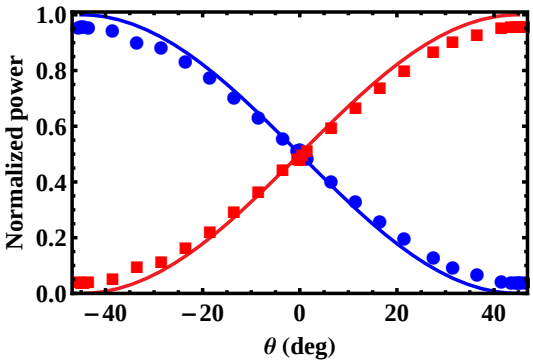

Fig. 3. Sorting of the OAM eigenstates $|\pm 2\rangle$. Dots ($\ell = 2$) and squares ($\ell = -2$) represent normalized intensities of the two exits of the final PBS in Fig. 1(c), as functions of the angle θ of the half-wave plate (HWP), that controls the state of the input beam. The solid line is given by $\sin^2(\theta - \pi/4)$ and $\cos^2(\theta - \pi/4)$, according to theory.

into the not entangled spin-orbit basis $|H, h_\ell\rangle$, $|V, v_\ell\rangle$, $|V, h_\ell\rangle$ and $|H, v_\ell\rangle$. The last states can be analyzed with standard techniques to measure the photon SAM and the OAM separately. The Bell state analysis gate can be realized by mounting the PSI-DP as a polarization C-NOT gate, as described in the previous section, to obtain $|B_1\rangle \to |A, v\rangle, |B_2\rangle \to |D, v\rangle, |B_3\rangle \to |A, h\rangle, |B_4\rangle \to |D, h\rangle$. Finally, a HWP at 22.5° can be used to rotate the photon polarization back into the horizontal plane.

2.2.3. Schmidt state generation

It is well known that any two-qubit state, such as the photon spin-orbit state, can be put into the general Schmidt form

$$|\Psi_S\rangle = \cos(\theta)|H, h_\ell\rangle - \sin(\theta)|V, v_\ell\rangle \tag{7}$$

by means of unitary transformations acting on each degree of freedom separately. Conversely, given the state [Eq. (7)], any spin-orbit state can be obtained by applying separate unitary transformations to the SAM and OAM degrees of freedom. The degree of entanglement of the

#132709 - $15.00 USD Received 2 Aug 2010; revised 9 Sep 2010; accepted 7 Oct 2010; published 10 Dec 2010

state [Eq. (7)] is parametrized by the angle θ. The non-maximally entangled state [Eq. (7)] could be used, for example, to demonstrate the Hardy paradox [37] – a test of the quantum nature of the entanglement and a proof of contextuality (or in the case of two-particles – non-locality) of quantum mechanics.

3. Experiment

Since quantum optics experiments that involve single-photon entanglement can be simulated using coherent CW laser source, to test experimentally our PSI-DP scheme we used a c.w. vertically polarized 532 nm TEM_{00} single frequency laser beam. To generate beams carrying nonzero OAM, we used the auxiliary setup shown in Fig. 1(b) based on the use of a q-plate (QP) [27,28]. The QP was placed after a set of quarter-wave plate $Q1$, half-wave plates $H1$, $H2$ and polarizer $P1$. Some of the optical components were removed or inserted back, depending on the desired photon state. Our QP had an unit topological charge and produced OAM eigenvalues of order $|\ell| = 2$. The action on the QP on the circular polarizations is given by [27]

$$\begin{aligned} |L,\ell\rangle &\xrightarrow{\widehat{QP}} \cos(\delta/2)|L,\ell\rangle - i\sin(\delta/2)|R,\ell+2\rangle, \\ |R,\ell\rangle &\xrightarrow{\widehat{QP}} \cos(\delta/2)|R,\ell\rangle - i\sin(\delta/2)|L,\ell-2\rangle \end{aligned} \tag{8}$$

where δ is the q-plate optical retardation. When the QP is tuned to a half-wave retardation ($\delta = \pi$) pure $\ell = \pm 2$ OAM eigenmodes are generated from a circularly polarized TEM_{00} input beam. In our experiments to test the PSI-DP the optical retardation δ of the q-plate was adjusted by thermal tuning [38]. Once tuned, the q-plate can generate any qubit in the $\ell = \pm 2$ OAM Hilbert subspace starting from an elliptically polarized TEM_{00}, according to [19]

$$\alpha|L,0\rangle + \beta|R,0\rangle \longrightarrow \frac{1}{\sqrt{2}}|H\rangle(\alpha|2\rangle + \beta|-2\rangle) \tag{9}$$

where a polarizer after the q-plate was used to select the H polarization. The insertion of the polarizer reduces the conversion efficiency upper limit to 50% of the incident photons [19,20]. The spin-to-OAM conversion process (STOC) in Eq. (9) is reversible and allows one to transfer back any OAM qubit into a corresponding polarization qubit according to

$$\alpha|H,2\rangle + \beta|H,-2\rangle \longrightarrow \frac{1}{\sqrt{2}}(\alpha|L,0\rangle + \beta|R,0\rangle). \tag{10}$$

The inverse STOC process is very useful in the detection stage, because the information encoded in the OAM degree of freedom is transferred into the light polarization, which is very easy to be analyzed. The auxiliary setup used for the OAM measurement is shown in Fig. 1(c). The photon state coming from the PSI-DP was first analyzed in polarization by the waveplates $WP2$ and PBS $P2$ and then the QP was used to transfer the OAM state into the corresponding polarization state of TEM_{00} mode [Eq. (10)], which was subsequently analyzed by waveplate $WP3$ and polarizer $P3$. The TEM_{00} mode in the output beam was selected by a spatial filter made by microscope objective and pinhole (not shown in the figure) [23]. The PSI-DP setup is shown in Fig. 1(a). At the PSI exit port the set of waveplates WP1 was inserted to compensate for the polarization changes due to the Dove prism, mirrors and PBS. The Dove prism, in particular, introduces a slight change in the light polarization [1–3, 39] so that a fraction of light exits from the wrong port, increasing the PSI-DP losses. A straightforward calculations for our Dove prism (BK7 glass, 45° base angles) shows, however, that the losses due to the light depolarization by the Dove prism do not exceed 2% at our rotation angles. The observed average overall transmittance of the PSI-DP was about 80%, so it is mainly due to scattering

#132709 - $15.00 USD Received 2 Aug 2010; revised 9 Sep 2010; accepted 7 Oct 2010; published 10 Dec 2010

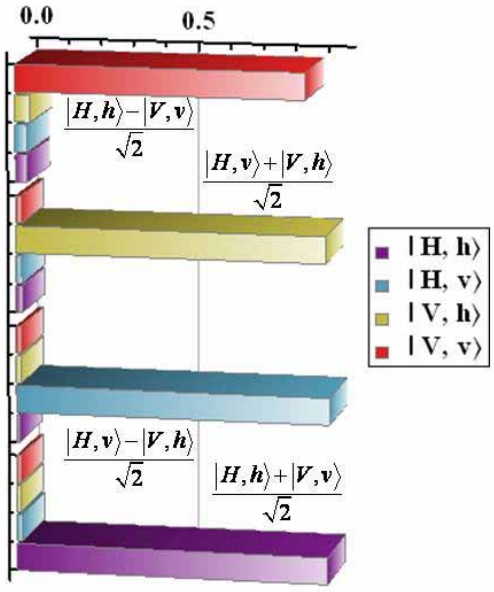

Fig. 4. Bell's state detection. The photons coming from the PSI-DP were first sorted by a PBS into their H and V polarizations and then sorted again by a QPs in each channel so to send the OAM h and v states into orthogonal polarizations and TEM_{00} mode by inverse STOC. The TEM_{00} mode was selected by a small aperture located beyond the QP.

and reflection losses from other optical components (we used no antireflection coating). We performed a few demonstrative experiments to test the different operations of the PSI-DP.

In the first experiment, we used the PSI-DP to clean up the TEM_{00} mode from the input beam (see Sec. 2.1.2). The input light was circularly polarized and sent into a QP. The optical retardation δ of the QP was changed so to obtain a mixture of $\ell = 0$ and $\ell = 2$ OAM eigenstates, according to Eq. (8). The polarizer $P1$ ensured antidiagonal polarization at the PSI input and the DP was rotated at $\alpha = \pi/8$. Figure 2 shows the data for the case $\ell = 2$. The $\ell = 2$ and $\ell = 0$ modes, shown in the figure, exit from the opposite ports of PBS $P2$ in Fig. 1(c). The measured contrast ratio of our cleaner was about 3.5:100.

In the second experiment, we used the PSI-DP to separate opposite OAM eigenstates. The input state was created by sending the H-polarized laser light into a HWP at angle $\theta/2$, a QWP at 45° and finally into a QP tuned for optimal STOC, so to obtain beyond the polarizer $P1$ of Fig. 1 the OAM qubit $|\Phi\rangle = \cos 2\theta|+2\rangle - \sin 2\theta|-2\rangle$ with antidiagonal polarization. After the QP tuning, the residual $\ell = 0$ component was negligible (less 1%). The OAM qubit superposition was changed by rotating the HWP. The DP in the PSI-DP was set at $\alpha = \pi/16$. The experimental results are shown in Fig. 3. The contrast ratio was 4.2:100 and the transmission efficiency larger than 90%, much larger than what can be obtained by holograms and spatial-filter combination.

In the third experiment, we implemented Bell's states detection with the PSI-DP. The states [Eq. (7)] can be generated with a QP with 100% efficiency. The states $|B_1\rangle$ and $|B_4\rangle$ are generated directly by sending in the QP a H and V-polarized TEM_{00} beam, respectively. The states $|B_3\rangle$ and $|B_2\rangle$ require an additional HWP at 45° beyond the QP, so to exchange the polarization states. The states [Eq. (7)] were disentangled by the PSI-DP C-NOT operation described in Sec. 2.2.1 with DP rotated at $\alpha = \pi/16$. The output base states $|H,h\rangle$, $|H,v\rangle$, $|V,h\rangle$ and $|V,v\rangle$

#132709 - $15.00 USD Received 2 Aug 2010; revised 9 Sep 2010; accepted 7 Oct 2010; published 10 Dec 2010

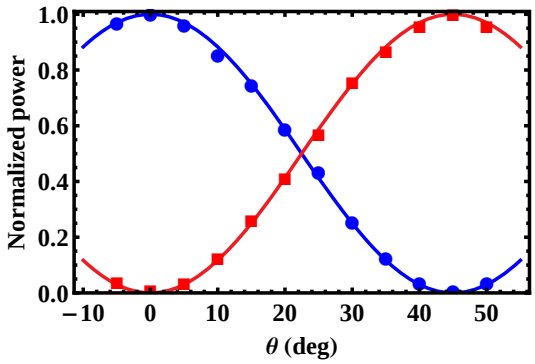

Fig. 5. Normalized intensities, corresponding to the $|H,h\rangle$ (dots) and $|V,v\rangle$ (squares) component of the state (7) as functions of the angle θ of the HWP. Solid lines correspond to $\cos^2(2\theta)$.

were analyzed in polarization and OAM separately by sending them into the four output channels of a setup formed by PBS and QPs with pinhole for inverse STOC. The average contrast ratio in separating the $|h\rangle$ and $|v\rangle$ OAM state by the inverse STOC was 1.4:100. The intensities of the signals at each one of the four exit gates of our analysis setup are shown in Fig. 4. At least 94% of the intensity was concentrated in one exit gate at once, showing very good disentanglement by the C-NOT PSI-DP operation.

In our final experiment, we used the PSI-DP to create the photon spin-orbit Schmidt state [Eq. (7)]. Although some photon spin-orbit states of the Schmidt form can be generated by simply sending through a QP an elliptically polarized TEM_{00} beam, this is not true for the state [Eq. (7)]. This is because some unitary operations, as $\pi/2$-conversion, for example, are difficult to be implemented in the OAM subspace and require cylindrical lens converters (the Dove prism performs a π-conversion). Our PSI-DP can do the OAM state $\pi/2$-conversion [30] and, hence, it can be exploited to create states as [Eq. (7)]. In our experiment, we first turned the laser beam polarization into diagonal and then sent it through the QP and PBS to obtain with 50% nominal efficiency the state $|H,d_\ell\rangle$, with $\ell = 2$, in our case. The state $|H,d_\ell\rangle$ was then made to pass through a HWP at angle θ and sent directly into the PSI-DP with Dove prism at $\alpha = \pi/8\ell = \pi/16$. A straightforward calculations shows that the photon spin-orbit state at the PSI exit is precisely the Schmidt state [Eq. (7)] with θ replaced by 2θ. The degree of entanglement of this spin-orbit state is controlled by rotating the HWP. We measured the intensity the $|H,h\rangle$ and $|V,v\rangle$ components of the Schmidt state generated by the PSI-DP with the same apparatus used for the SAM and OAM analysis in the previous experiment on Bell states. The results are reported in Fig. 5.

For the sake of completeness we measured by full spin-orbit tomography the density matrix of one of the states with maximal spin-orbit entanglement. The tomographic technique is commonly used in single photon quantum optics to measure qubits [40] and can be used also to characterize OAM photon states or even spin-orbit photon states [21, 30, 41]. The main advantage of tomography is that both the amplitude and phase of the optical field can be retrieved without having recourse to interferometers.The basic idea is to measure the Stokes parameters $s_i (i = 1,\ldots,3)$ by intensity differences in the left/right circular basis, in the horizontal/vertical basis and in the antidiagonal/digonal basis for the polarization qubit and in similar bases for the OAM qubit [40]. In our measurements the tomography was carried out by using PBS and QPs with pinhole for inverse STOC as in the previous experiments. The results are shown in Fig. 6 and are in excellent agreement with theory. The measured average fidelity defined as

#132709 - $15.00 USD Received 2 Aug 2010; revised 9 Sep 2010; accepted 7 Oct 2010; published 10 Dec 2010

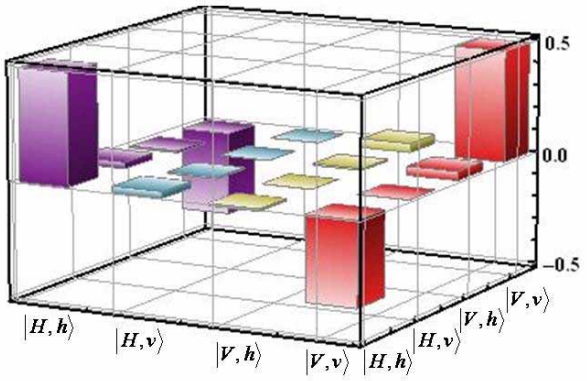

Fig. 6. Density matrix of the maximally entangled Hardy state, reconstructed by full spin-orbit tomography

the squared scalar product of the observed spin-orbit state and the expected state [Eq. (7)] was 92%.

4. Conclusions

In conclusions, we introduced a new interferometric layout, a Polarizing Sagnac interferometer with a Dove prism, that can realize OAM state sorting and different spin-orbit quantum gates at the single photon level. The PSI-DP is more stable than Mach-Zehnder-based interferometers for OAM because of the self-compensated optical paths and it is easier to use because it requires only one Dove prism. Moreover the PSI-DP can do nontrivial operation in the spin-orbit space, as experimentally demonstrated by few examples. Useful applications of the PSI-DP as an OAM sorting device and as a realization of quantum unitary gates, such as OAM C-NOT gate, full Bell's states detection gate, and a gate to generate Schmidt's photon states with controllable spin-orbit entanglement have been realized in this work, but we are confident that many other will be surely envisaged in the near future.

Acknowledgments

We thank Ebrahim Karimi for help in the quantum tomography analysis and useful discussions. The project PHORBITECH acknowledges the financial support of the Future and Emerging Technologies (FET) programme within the Seventh Framework Programme for Research of the European Commission, under FET-Open grant number: 255914.

#132709 - $15.00 USD Received 2 Aug 2010; revised 9 Sep 2010; accepted 7 Oct 2010; published 10 Dec 2010